Revista de la Construcción
ISSN: 0717-7925
revistadelaconstruccion@uc.cl
Pontificia Universidad Católica de Chile
Chile

Cabrera-Covarrubias, Francisca Guadalupe; Gómez-Soberón, José Manuel; Almaral-Sánchez, Jorge Luis; Arredondo-Rea, Susana Paola; Corral-Higuera, Ramón

Mechanical properties of mortars containing recycled ceramic as a fine aggregate replacement

Revista de la Construcción, vol. 14, núm. 3, diciembre, 2015, pp. 22-29
Pontificia Universidad Católica de Chile
Santiago, Chile

Available in: http://www.redalyc.org/articulo.oa?id=127643355003

Mechanical properties of mortars containing recycled ceramic as a fine aggregate replacement

Propiedades mecánicas de morteros que contienen cerámica reciclada como reemplazo del árido fino

Francisca Guadalupe Cabrera-Covarrubias (Main Author)
Universidad Politécnica de Cataluña, Escuela Técnica Superior de Ingenieros de Caminos, Canales y Puertos de Barcelona, España.
francisca.guadalupe.cabrera@estudiant.upc.edu

José Manuel Gómez-Soberón (Contact Author)
Universidad Politécnica de Cataluña, Escuela Politécnica Superior de Edificación de Barcelona.
Av. Doctor Marañón 44-50, 08028 Barcelona, España.
+34 934016242
josemanuel.gomez@upc.edu

Jorge Luis Almaral-Sánchez
Universidad Autónoma de Sinaloa, Facultad de Ingeniería de Los Mochis, Mexico.
jalmaral@uas.edu.mx

Susana Paola Arredondo-Rea
Universidad Autónoma de Sinaloa, Facultad de Ingeniería de Los Mochis, Mexico.
paola.arredondo@uas.edu.mx

Ramón Corral-Higuera
Universidad Autónoma de Sinaloa, Facultad de Ingeniería de Los Mochis, Mexico.
ramon.corral@uas.edu.mx

Manuscript Code: 225
Date of Reception/Acceptance: 01-07-2014 / 01-12-2015.

Abstract
We study the behavior of mortars where 0%, 10%, 20%, 30%, 50% and 100% of their original natural sand was replaced by ceramic sand in a search of potential new building materials that will help to conserve natural resources and that are environmentally friendly. In this paper, the physical properties of the sands and their derived mortars, including their compressive strength, flexural strength, and shrinkage due to base and total drying, are characterized. Our results show that the compressive and flexural strengths of the recycled mortars decrease proportionally to the amount of natural sand replacement used. A similar behavior is observed for the shrinkage due to drying in mortars with low ceramic substitutions (10%, 20% and 30%). Based on these findings, we believe that the use of mortars made with recycled sand (with substitution contents lower than 30%) could be feasible in applications where the mechanical requirements are low.

Keywords: recycled mortars, ceramic materials, mortar shrinkage

Resumen
A partir de la búsqueda de nuevas alternativas en el área de construcción que ayuden a la conservación de los recursos naturales y del medio ambiente, se estudia el comportamiento de morteros con sustituciones parciales de reemplazo del 0%, 10%, 20%, 30%, 50% y 100% de arena cerámica reciclada por arena natural. Se caracterizan las propiedades físicas de las arenas estudiadas, así como las propiedades mecánicas de los morteros resultantes de ellas; tales como la resistencia a la compresión, flexión y de retracción básica, por secado y total. Los resultados obtenidos indican que para la resistencia a compresión y a flexión de los morteros reciclados, éstos sufren decrementos proporcionales al remplazo de la arena natural; sin embargo, para el caso de la retracción por secado éstos reportan comportamiento similar (morteros con sustituciones bajas de 10%, 20% y 30%). En base a lo anterior, morteros con arena cerámica reciclada (con contenidos menores al 30% de reemplazo) podrían ser factibles de su utilización en aplicaciones, en las cuales los requerimientos de éstos sean bajos.

Palabras Claves: morteros reciclados, materiales cerámicos, retracción morteros

Introduction

Environmental awareness driven by climate change and the reduction of natural resources is stimulating the search for new alternatives aimed to reduce the use of natural resources (Barluenga & Hernández-Olivares, 2004; Bektas, et al., 2009; Cabrera Álvarez et al. 1997; Lopes Lima & Batista Leite, 2012; Shui et al., 2008; Tam et al., 2007).

The current increase of civil projects in the construction sector has generated a large amount of residues, called residues from construction and demolition (RCDs) (Calvo Pérez et al., 2002; Echevarría Caballero et al., 2005; Jiménez et al., 2013; Parra y Alfaro et al., 2006). Residues derived from the demolition of buildings could be used as replacement materials for natural aggregates.

This replacement could both mitigate the sustainability problem and result in direct environmental and economic benefits (Jiménez et al., 2013; Lee, 2009; Lehmann, 2011; Miranda & Selmo, 2006; Pereira-de-Oliveira et al., 2012; Sales & Rodrigues de Souza, 2009; Tam et al., 2007; Wang & Tian, 2009)

Dump waste materials could be used in new applications, such as the fabrication of concretes and mortars (V. Corinaldesi et al., 2002; Valeria Corinaldesi, 2012; Dapena et al., 2011; Gutiérrez Moreno et al., 2015; Tertre, 2007; Vegas et al., 2009) after an adequate selection process, including specific grinding and proper sieving.

Some of the feasible RCD components suitable for recycling as replacements for aggregates in recycled mortars are materials containing ceramic elements. Mortars with applications in construction are formed by an important fraction of fine aggregates (i.e., sand), among other components.

Traditionally, these materials are natural sands extracted from quarries and rivers, so their use has an environmental impact and leads to their exhaustion because they are non-renewable materials. Thus, the use of recycled sands originating from ceramic materials in mortar fabrication could be an alternative for current and future sustainable construction.

Therefore, the goals of this work are to analyze the physical and mechanical properties and deferred deformation of recycled ceramic mortars (CMs) with different percentages of recycled sand derived from ground ceramic residues as substitutes for their original contents of natural sand. The aim of this analysis is to verify the effect of substituting natural materials by recycled ones on the behavior of CMs, determining the criteria for their optimal use in potential applications, and reporting data on their exhibited properties.

Materials

The recycled ceramic aggregates (CAs) used in this work came from local industries and were certified in their processing. The minimum particle size of the fine aggregates was 0-5 mm, and they were derived from defective residues of ceramic roof tiles that did not comply with technical size and geometry specifications.

Silica sand, which was acquired from a local marketer and had a particle size of 0-4 mm, was used as natural sand or natural aggregate (NA).

Figure 1 shows the CA (a) and NA (b) used in this work, depicting some of the visual differences existing between them, such as the (evident) color, the maximum particle size (higher for CA), and the particle size distribution.

Both sands required adjustments to their granulometric profiles so their respective particle size distributions could be brought (as much as possible) into compliance with the specifications of the ASTM C144 standard. If such adjustments were not performed, both granulometric profiles would be unbalanced (i.e., the particle size distributions would have steep hikes, sharp changes in curvature, or distribution curves far from the limits established by industry standards), implying that the obtained results could be a consequence of different profiles rather than different materials.

To ensure that the particle size distributions were properly adjusted, a criterion for combining the different percentages of each aggregate type was developed, which consisted of using two different fractions of different particle sizes (both from the original material of each sand) that were separated by a No. 30 sieve (0.59 mm). This criterion is based on the attempt to achieve suitable compositions, with minimal intervention, that generate similar profiles that are close to the limits of regulation.

To achieve that similarity, the No. 30 sieve was identified as the best means to attain the targeted particle size (i.e., the particle size distribution tail corresponding to smaller sizes that caused the particle size to fall outside the limits of the regulation). If such resulting fractions are combined into different percentages (for each profile under study, CA and NA) and equal targets are required (maximum capacity), then the resulting profiles of each sample produce similar granulometric curves that are close to the limits described in the standards.

This approach avoids introducing variables that could be related to a profile divergence during our research; however, for industrial applications, we acknowledge the existence of such a limitation. The maximum capacity for the CA was achieved by a combination of 60% sand with particle sizes bigger than the No. 30 sieve (0.59 mm) and 40% sand with particles sizes smaller than it. For the NA, the optimum combination was found for mixtures of 50% of each of the fractions separated by the No. 30 sieve (0.59 mm).

Figure 1. Sands used (cm): a) CA, b) NA. Source: Self-elaboration.

a)

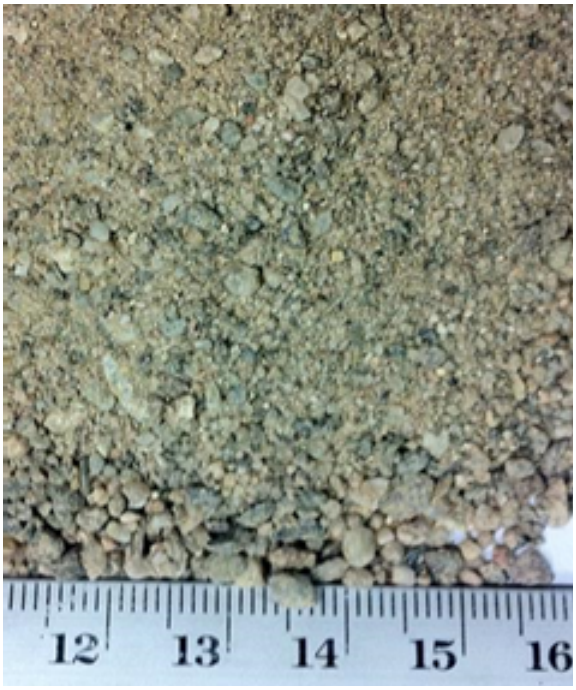

b)

Figure 2 shows the granulometric curves of both sands resulting from the above granulometric adjustment, together with the extreme limits established by the standard. As depicted, for the CA, 33% of the sample falls below the lower limit of the standard (between mesh No. 16, 1.19 mm, and No. 8, 2.38 mm), while only 4% of the sample falls below the lower limit for the NA.

Even when both curves are not optimal (in practice, optimal curves are impossible to achieve), the adjustment will ensure that the particle size distribution will not be an important factor affecting the study of aggregate replacement in either sand.

Figure 2. Granulometric profile of used sands. Source: Self-elaboration.

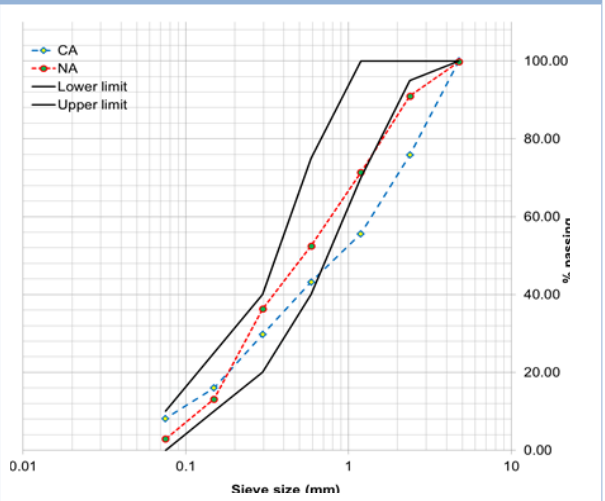

Some of the physical properties of the sands are described in Table 1. In general, compared to the NA, the CA has a lower density (29.5 and 17.8% lower density in terms of the OD (oven-dry condition) and the SSD (saturation-surface-dry condition), respectively) and exhibits a notably higher absorption capacity (differing by 16.8%).

The behavior of volumetric weights agrees with the reported values derived from their densities: the values for the CA are smaller than those for the NA (31.9 and 24.8% lower bulk density in terms of OD and SSD, respectively), and there is a greater void content in the CA (7.3% higher than that in the NA). The causes for such behaviors could be related to the inherent low densities of the components and their exhibited unbalanced granulometric profiles, with a higher amount of coarse aggregates (i.e., a higher fineness modulus), which hinders their achievement of an optimal compactness.

Table 1. Physical properties of aggregates. Source: Self-elaboration.

Property*	CA	NA
Density (OD) (kg/m3)	1820.9	2581.6
Density (SSD) (kg/m3)	2155.4	2623.6
Bulk density (OD) (kg/m3)	1182.0	1735.1
Bulk density (SSD)(kg/m3)	1399.1	1860.8
Voids (%)	35.3	32.9
Water absorption (%)	18.4	1.6
Fineness modulus	2.8	2.4
Materials Finer that 75-µm (sieve No. 200) (%)	8.2	2.9

* Determined according to ASTM.

Finally, Portland cement classified as CEM I 42.5 N/SR (UNE EN 197-1:2011, by its usual properties and components) mixed with tap water without any further treatment or load was used as a binding agent.

Experimental Works

Mortar specimens of 4 cm x 4 cm x 16 cm with substitutions (change factor "R" = [CA/total aggregates] x 100, in weight) of 0%, 10%, 20%, 30%, 50% and 100% of the original NA content by CA were prepared to evaluate their compression and flexural behaviors. Specimens 2.5 cm x 2.5 cm x 28.5 cm in size were used to evaluate shrinkage. All of the mixtures were designed with a cement/sand ratio of 1:4 (by weight) and an initial water/cement (w/c) fraction of 0.5.

The w/c fraction was corrected according to the ASTM C203 standard until a fluidity of 110 ± 5% was achieved, according the ASTM C109 standard. The water increments reported in the recycled mixtures were a consequence of the individual needs of each mixture, given the influence of the CA content.

To achieve these compositions, the CA and the NA were taken to their saturation points (by mixing with water for 1 minute) before the cement was added to the mixer. The characteristics and ratios used to manufacture 1 dm3 of each of the mixtures studied are shown in Table 2.

Table 2. Features and mixture proportions study. Source: Self-elaboration.

Materials (g)		Replacement level of fine recycled aggregate					
		R = 0	R = 10	R = 20	R = 30	R = 50	R = 100
Cement		400	433	381	372	348	323
NA**	<sieve 30	800	780	610	521	348	0
	>sieve 30	800	780	610	521	348	0
CA**	<sieve 30	0	69	122	179	278	517
	>sieve 30	0	104	183	268	417	775
Water* (w/c)		0.84	0.90	0.93	1.00	1.14	1.48

*Necessary water for mixed = water of hydration +water to saturate aggregates + water for workability.

**Dry condition.

Assays details

Density and porosity

The apparent densities, the open porosities, and the mortar absorptions were evaluated using half of the specimen remaining from the assay before the flexural test (UNE EN 1015-10 and EN 1936) at an age of 60 days (because this is the most representative maturity age for referencing mixtures with long-term tests). The cracked face resulting from the flexural test was matched to the other face to improve this assay's approximation.

Compressive and flexural strengths

The assay ages established for these tests were 3, 7, 28, 60 and 90 days. The specimens were maintained in saturation conditions by keeping them immersed in water until the age of the test was reached, when the specimens were removed from the water bath and immediately tested. The time elapsed between the specimen removal and testing was never longer than 30 minutes.

Three specimens for each variable were used during the flexural tests, following the guidelines of the ASTM C348 standard. One of the halves (3 specimens per variable) remaining from the flexural tests was subsequently used for the compressive tests according to the suggestions of the ASTM C349 standard.

Shrinkage

To characterize shrinkage (due to base, drying, and total shrinkage), six specimens with sizes of 2.5 cm x 2.5 cm x 28.5 cm were fabricated for each of the conditions being studied. Immediately after their removal from the cast, they were prepared according the guidelines described in previous studies (Gómez-Soberón, 2002);(Gómez-Soberón, 2003).

Three of the six specimens were covered by three layers of paraffin and aluminum foil to evaluate the basic shrinkage (εbasic), and the remaining three were used for total retraction

(εtotal) (see Figure 3a).

By computing the difference between these two values, we deduced the shrinkage due to drying (εdrying) of the mortars. The first reading for the shrinkage was taken after 24 hours of mixing; then the specimens were placed in a curing chamber for 28 days, and the following readings were taken on days 3, 7, 14 and 28 (removing them from the curing chamber only for the reading).

After this period, the specimens were removed from the chamber and exposed to the laboratory ambient conditions (T = 23 °C and RH = 50%), and readings were subsequently taken at ages of 3, 7, 14, 28, 40, 60 and 90 days. The recordings were taken using equipment with a rigid test-frame (Figure 3b) and a micrometer with a precision of 0.001 mm (Figure 3c), according to the suggestion by the ASTM C490-04 standard.

Figure 3. a) Basic and total shrinkage specimen, b) the test frame, c) the micrometric reader. Source: Self-elaboration.

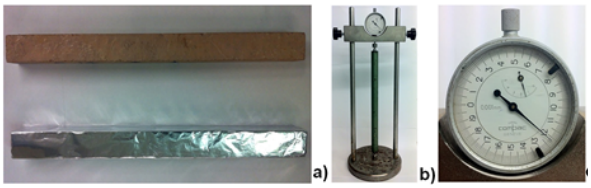

Results And Discussion

Density and porosity

The physical properties of the hardened mortar are shown in Figure 4. The CMs exhibited lower values for apparent density than the mortars made with natural sand (NAT), and the density was inversely correlated with R. These variations ranged from -0.1% for CM10 up to a maximum of -21.5% for CM100, with respect to NAT in both cases. This behavior could be explained by the low density of the CA compared with the NA (see Table 1), which also has been reported in previous studies (Jiménez et al., 2013; J. Silva, Brito, & Veiga, 2010; M. A. G. Silva, Silva, & Simão, 2007).

On the other hand, the CM porosity and absorption values are inversely correlated with the apparent densities of the specimens. The more noticeable differences with NAT occur with higher R factors, at values of 115.7% for porosity and 115.3% for absorption for CM100. In the case of CM absorption, these results could be related to the high absorption capacity of the CA used for fabrication (see Table 1).

Regarding porosity, the observations may be related to a higher requirement for water during the mixing procedure (see Table 2), with respect to the amount retained by the CA, and the evaporation of water could leave behind a bigger network of voids in the CMs. It is possible that the characteristics specific to aggregates, such as the sharp forms of the CA or their particle size distributions, could also concurrently modify the workability of the CM.

This effect, in turn, results in a higher water demand (i.e., the sharper-edged particles observed in the CA) for a desired consistency.

Figure 4. Density, porosity and absorption of the CM. Source: Self-elaboration.

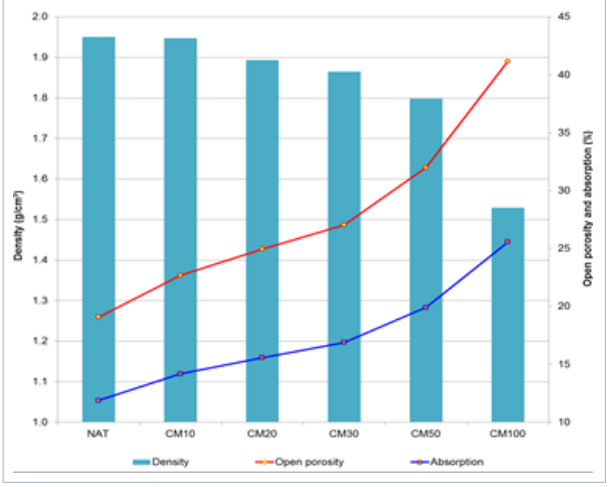

Compression strength

Figure 5 shows that the resistances of all of the mixtures increased over the elapsed time, probably due to hydration reactions occurring in the mortars; however, comparing CM with NAT, the resistances decrease. This behavior is observed at ages of 3, 7 and 90 days; at 90 days, the CM20 mixture showed the highest values of all the CMs tested (30.54 MPa).

However, at ages of 28 and 60 days, the behavior of CM10 surpasses even that of the NAT (thus indicating a possible null effect of the substitution of the CA), increasing its values by 1.6 and 3.8%, respectively (an average of 2.72%), which nevertheless could be considered to be low changes or changes related to the dispersion.

In general, the behavior of resistance loss related to increasing the CA content could be caused by the physical characteristics of the CAs, such as lower densities and higher absorptions than those exhibited by the NA. The NA mixtures end up producing weaker mortars that form more porous matrices due to their higher water requirements.

Along the same lines, it is also possible that the shape and form of the particles could affect their adherence to cement. Similar behaviors have been reported previously in where the characteristics of the CA (low density and high absorption) have been indicated as responsible (Valeria Corinaldesi, 2012); as well as to the variations to the relationship w/c due to the high absorption of the CA (João Silva ET AL., 2009),and also the dosage method used (by volume) (Jiménez et al., 2013).

The reasons for the higher resistances of the CMs with respect to the NAT have not been experimentally validated; however, we predict that one plausible hypothesis for this behavior could be that their pozzolanic reactivities (associated with the fine fraction in CA) promote the “filling effect” in the mortar matrix.

Previous works have reported that CAs with percentages below 30% (and in some cases even up to 50%) exhibit compression strengths equivalent to or even higher than those of the reference mixture. Such behavior is justified by the pozzolanic reactivity that such aggregates can exhibit, thus generating new crystalline products that improve the mortar matrix (Jiménez et al., 2013; Kumavat & Sonawane, 2013; Silva et al., 2010).

Figure 5. Compressive strength of CM with respect to age. Source: Self-elaboration.

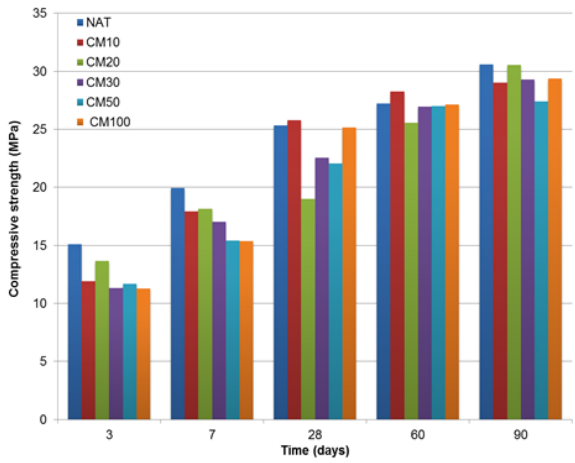

Figure 6. Evolution of hydration with the age of the CM based on the compressive strength. Source: Self-elaboration.

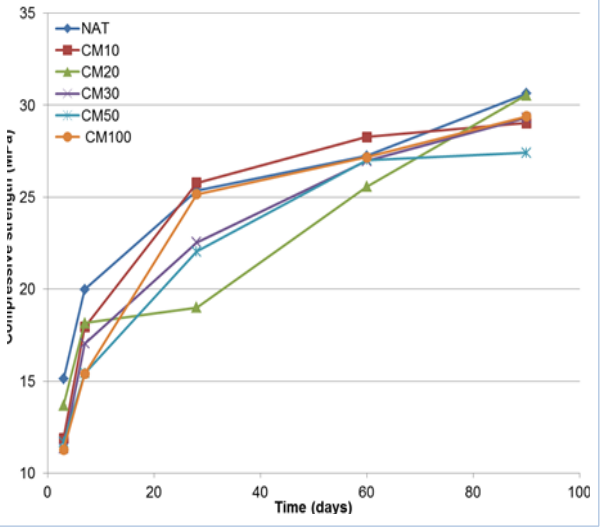

Regarding the change in resistance of the mortars (Figure 6), even when there are some variations between the CMs and NAT, the curves of all of the CMs behave similarly. This similarity shows that the hydration process follows a consistent pattern for CMs; that is, the compressive strength increases with time, but, for ages close to 28 days, the values tend to stabilize (that is, the increase in resistance decelerates).

Flexural strength

Figure 7a shows that the flexural strength behavior is similar to the behavior observed for the compression strength, which tends to increase in all the mixtures with time. However, the strengths of the CMs decrease in the presence of CAs, and they respond to an increasing R factor for all of the analyzed ages. At the ages of 3 and 7 days, CM20 exhibits strength values similar to those of NAT, with differences of -4.7% and -1.9%, respectively.

This result suggests that mortars with such percentages of ceramic materials could develop resistances equivalent to those exhibited by NAT. For the age of 28 days, CM10 and CM30 are most similar to NAT (-10.3% and -11.7%, respectively). Finally, after 90 days, CM30 is the most similar (8.5%) to NAT. The highest strength loss among the CMs is reported for CM100, with a curing age of 90 days, which could decrease up to 19% with respect to NAT. On the other hand, CM30 aged for 60 days exhibits the lowest strength loss (of only -1.2%).

In general, the observed loss of flexion strength related to the increase of CAs can be explained by the physical characteristics of the CAs (similar to the cause for the change in compression strength in the CM): a lower density and a higher absorption are observed in mortars with a porous matrix, along with a possible deficient adherence between the cement and the aggregates.

Similar behaviors have been reported in previous works for samples with substitution percentages of 100% CA (Valeria Corinaldesi, 2009) (Valeria Corinaldesi, 2012), where such behavior was related to the low density of the specimens and the observed CA porosity (acknowledged as the weakest link of the set). In addition, the same work suggests that the effect of the "matrix filling" caused by the pozzolanic addition of fine particles may not control the overall behavior of specimens with high CA contents.

The hydration capacity increased for all of the samples (see Figure 7b). Based on the results obtained for the extremes cases under study (3 and 90 days), we found that CM30 had the most accelerated evolution of hydration capacity, representing a difference of only 1.1% with respect to NAT. On the other hand, the material with the worst hydration evolution was CM100 (16.7% with respect to the samples with natural sand).

As a partial conclusion, the results presented here are not conclusive regarding the relationships found for the different percentages, but they are indeed conclusive for the cases with maximum substitution (100%). To justify this conclusion, we note that these decreases are related in a direct way to the fact that in specimens with high CA contents, the possible pozzolanic effect could be attributed to higher strengths, as was observed in other works (João Silva et al., 2009), which might not be sufficient to induce changes in the cement matrix. Therefore, the physical properties of CAs (the density, high absorption and higher porosity) are responsible for the weakness observed in the CM.

Shrinkage

To study the deformations in the CMs, the obtained curves were divided into two stages: a) data obtained in a curing chamber, in the age (t) range of $0 < t < 28$ days; and b) data obtained in the laboratory environment, ranging from $28< t < 90$ days. During the first stages (in the humidity chamber) and during the process of basic shrinkage ($\varepsilon basic$) (Figure 8a), the mortars CM10, CM20, CM30 and NAT shrank, but CM50 and CM100 actually expanded (all of them were covered with paraffin and are referenced in the plot with the term PAR).

Analyzing the behavior of the previously discussed variables, for the first set, we could predict that the high absorption observed by the CAs with a low amount of CM substitution provides a low amount of water for the hydration process, which produces a chemical reaction that consumes water. On the other hand, the observations obtained for the second set of variables could be explained by the high w/c ratio values required for the CMs; given that high CA substitutions lead to elevated absorption capacities, these materials will have highly porous networks for the hydration process.

The associated high amount of available water therefore induces the generation of CSH products that are known for inducing specimen expansion.In the same stage but during the process of total shrinkage ($\varepsilon total$) (Figure 8b), all of the specimens exhibited expansive deformation values at the end of their exposure periods inside the curing chamber. Such behavior could be explained by the specific curing conditions

(i.e., a high relative humidity and a constant temperature) that stimulate water inclusion in the specimens, with the consequent higher sensitivity and correlation with the R factor.

During the second stage (in the laboratory environment), it was necessary to set aside the values obtained in the first deformation stage (in the curing chamber, both for εbasic and εtotal) so the real values describing deformation in the laboratory environment could be obtained. We defined the value of both the obtained deformation and the curing age as zero at the beginning of the drying stage (in the laboratory environment); that is, ε28 days= 0% and t28 days = 0.

Figure 9a shows the curves for εbasic (only for the laboratory environment) and indicates that at t = 90 days, CM50 and CM100 were located in the expansion zone, while the others, CM10, CM20, CM30 and NAT, were in the shrinkage zone. This behavior can be understood as a continuation of the tendency explained before (a curing period in a curing chamber), supporting the assumption that the laboratory conditions do not affect the specimens (at least for 40 < t < 50 days).

At this time, however, CM50 and CM100 exhibited an "interruption" in their expansive processes, then starting a new trend that was not increasing and instead constant (i.e., horizontal). The curves for all of the other CMs and for NAT tend toward shrinkage values, with CM10 and CM20 being the steepest curves. Based on this information, the behavior of the CM could be significantly affected by a desiccation process starting from t > 50 days.

Curves for εtotal are shown in Figure 9b. In this figure, all of the CM and NAT cases show remarkable and similar deformation values. The observed behavior can be summarized by mentioning that at the beginning of the new environmental conditions (a low RH and a high temperature), all of the specimens suffer drastic shrinkage deformations (max εtotal = 0.1081% for CM10 between 0 < t < 30 days). Water loss from the CM porous networks that reduces the interstitial tension is most likely the cause of this shrinking behavior.

During the period between 40 < t < 50 days, the majority of the curves exhibit a constant linear tendency of no deformation, with exception of CM20, which is the only specimen where deformation continues. This behavior can be explained by noting that in this timeframe, the effect of the laboratory environment compensates for CM deformation and limits the availability of water for extraction.

From the difference between εtotal and εbasic, it is possible to obtain the shrinking due to drying (εdrying) (see Figure 10). Here, CM50 and CM100 for t = 90 days are the specimens with the highest deformations (εdrying = 0.0986% and 0.1141%), which were 24% and 44% higher than those of NAT. Similar values (43%) were also reported for mortars with 100% ceramic sand (at t = 80 days) (J. Silva et al., 2010). Regarding CM10, CM20 and CM30, the observed values were similar to the values exhibited by NAT (absolute differences of only 0.0084%, 0.0054%, and 0.0089%). In other works, similar deformation values were reported (t = 56 days) for mortars containing 10% and 20% recycled sand (Bektas et al., 2009).

The behavior of the first set (CM50 and CM100) can be explained by their more porous networks, which are interconnected and open. These networks exhibit reduced pressures because of the presence of water inside them, allowing water to evaporate when the specimens are exposed to more extreme conditions of temperature and humidity.

On the other hand, the rest of the samples (CM10, CM20, and CM30), containing "equivalent" porous networks, exhibited "stability" towards deformation once the available water was depleted at the environmental conditions that the specimens were exposed to. A complementary hypothesis explaining the behavior of the CMs is attributed to the high water requirement of the CMs and to an elevated absorption by the CA, which facilitates water extraction in dry environments (Wang & Tian, 2009) and, in extreme conditions, induces cracking (Bektas et al., 2009) (Vegas et al., 2009).

Conclusions

Based upon the results obtained in this work, the following conclusions can be reached:Due to the higher absorption exhibited by CA, the CMs need a higher amount of water to achieve equivalent workabilities to make them adequate to use, especially if they are initially mixed with dry sand.

The CMs exhibited compression and flexion strengths smaller than those of NAT (t = 90 days); of the CMs, CM20 showed the highest compression strength (30.54 MPa), while CM30 had the highest value of flexible strength (8.55 MPa). Such decreases in resistance does not imply that they should not be used but rather be considered as feasible alternatives for applications with reduced mechanical requirements.

CM10, CM20, and CM30 (t = 90 days) exhibit a εdrying behavior similar to that of NAT, with a difference of only 0.01%, implying that these reduced CA percentages could lead to deformations in the CM, which is the opposite case for elevated CA substitution percentages. In summary, we can conclude that CM10, CM20 and CM30 have demonstrated the capacity to achieve shrinkage levels and compression and flexible strengths that are acceptable to be considered as feasible alternatives consistent with environmental conservation.

Figure 10. εdrying of the CM. Source: Self-elaboration.

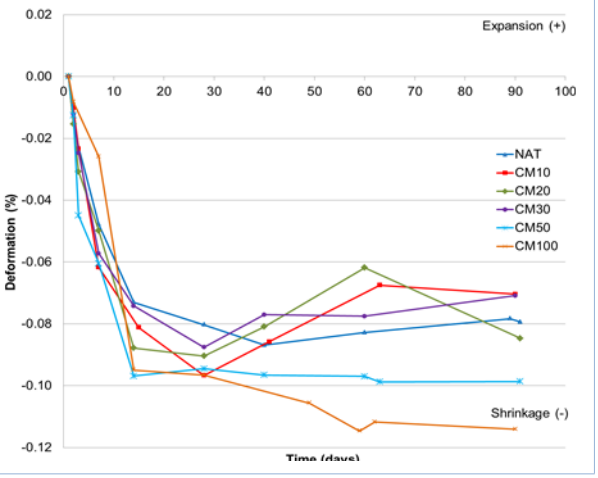

Acknowledgements

The authors thank CONACYT for its doctoral scholarship program, the Polytechnic Higher School of Building Construction of Barcelona-UPC, the Department of Architectonic Constructions II-EPSEB-UPC, the School of Engineering Mochis-UAS and, finally, the program of Young Doctors-UAS.

References

Barluenga, G., & Hernández-Olivares, F. (2004). Experimental approach to the use of recycled materials in mortar and concrete for architectural experimental applications. In E. Vázquez, C. F. Hendriks, & G. M. T. Janssen (Eds.), International RILEM Conference on the Use of Recycled Materials in Building and Structures (pp. 403–411). RILEM Publications SARL.

Bektas, F., Wang, K., & Ceylan, H. (2009). Effects of crushed clay brick aggregate on mortar durability. Construction and Building Materials, 23(5), 1909–1914. doi:10.1016/j.conbuildmat.2008.09.006

Cabrera Álvarez, J. L., Urrutia, F., Lecusay, D., & Fernández, A. (1997). Morteros de albañilería con escombros de demolición. Materiales de Construcción, 47(246), 43–48.

Calvo Pérez, B., Parra y Alfaro, J.-L., Astudillo Matilla, B., Sanabria Zapata, C. M., & Carretón Moreno, R. (2002). Áridos Reciclados para Hormigones y Morteros. Caracterización Mineralógica y Química.ingenierosdeminas.org. Retrieved from http://ingenierosdeminas.org/documentos/06-Materias primas de interes industrial.-3.pdf

Corinaldesi, V. (2009). Mechanical behavior of masonry assemblages manufactured with recycled-aggregate mortars. Cement and Concrete Composites, 31(7), 505–510. doi:10.1016/j.cemconcomp.2009.05.003

Corinaldesi, V. (2012). Environmentally-friendly bedding mortars for repair of historical buildings. Construction and Building Materials, 35, 778–784. doi:10.1016/j.conbuildmat.2012.04.131

Corinaldesi, V., Giuggiolini, M., & Moriconi, G. (2002). Use of rubble from building demolition in mortars. Waste Management, 22(8), 893–899. Retrieved from http://www.ncbi.nlm.nih.gov/pubmed/12423051

Dapena, E., Alaejos, P., Lobet, A., & Pérez, D. (2011). Effect of Recycled Sand Content on Characteristics of Mortars and Concretes. Journal of Materials in Civil Engineering, 23(4), 414–422. doi:10.1061/(ASCE)MT.1943-5533.0000183.

Echevarría Caballero, M., Sanabria Zapata, C. M., & Parra y Alfaro, J. L. (2005). Fabricación de morteros con árido reciclado. Ingeopres: Actualidad Técnica de Ingeniería Civil, Minería, Geología Y Medio Ambiente, (141), 26–28. Retrieved from http://europa.sim.ucm.es/compludoc/AA?articuloId=424089

Gómez-Soberón, J. M. V. (2003). Relationship Between Gas Adsorption and the Shrinkage and Creep of Recycled Aggregate Concrete. Cement, Concrete and Aggregates, 25(2). doi:10.1520/CCA10442J

Gómez-Soberón, J. M. V. (2002). Porosity of recycled concrete with substitution of recycled concrete aggregate - An experimental study. Cement and Concrete Research, 32(8), 1301–1311. doi:10.1016/S0008-8846(02)00795-0

Gutiérrez Moreno, J. M., Mungaray Moctezuma, A., & Hallack Alegría, M. (2015). Reuse of Hydraulic Concrete Waste as a New Material in Construction Procedures : a Sustainable Alternative in Northwest Mexico. Revista de La Construcción, 14(2), 51–57. doi:10.4067/S0718-915X2015000200007

Jiménez, J. R., Ayuso, J., López, M., Fernández, J. M., & Brito, J. de. (2013). Use of fine recycled aggregates from ceramic waste in masonry mortar manufacturing. Construction and Building Materials, 40, 679–690. doi:10.1016/j.conbuildmat.2012.11.036

Kumavat, H. R., & Sonawane, Y. N. (2013). Feasibility Study of Partial Replacement of Cement and Sand in Mortar by Brick Waste Material. International Journal of Innovative Technology and Exploring Engineering (IJITEE), 2(4), 17–20.

Lee, S.-T. (2009). Influence of recycled fine aggregates on the resistance of mortars to magnesium sulfate attack. Waste Management, 29(8), 2385–2391. doi:10.1016/j.wasman.2009.04.002

Lehmann, S. (2011). Optimizing Urban Material Flows and Waste Streams in Urban Development through Principles of Zero Waste and Sustainable Consumption. Sustainability, 3(1), 155–183. doi:10.3390/su3010155

Lopes Lima, P. R., & Batista Leite, M. (2012). Influence of CDW Recycled Aggregate on Drying Shrinkage of Mortar. Open Journal of Civil Engineering, 2(2), 53–57. doi:10.4236/ojce.2012.22009

Miranda, L. F. R., & Selmo, S. M. S. (2006). CDW recycled aggregate renderings: Part I – Analysis of the effect of materials finer than 75µm on mortar properties. Construction and Building Materials, 20(9), 615–624. doi:10.1016/j.conbuildmat.2005.02.025

Parra y Alfaro, J. L., Astudillo Matilla, B., Carretón Moreno, R., Castilla Gómez, J., Sanabria Zapata, C. M., & Antuña Bernardo, E. (2006). Áridos reciclados para hormigones y morteros. Boletín Geológico Y Minero, 117(4), 763–772. Retrieved from http://dialnet.unirioja.es/servlet/articulo?codigo=2264832

Pereira-de-Oliveira, L. A., Castro-Gomes, J. P., & Santos, P. M. S. (2012). The potential pozzolanic activity of glass and red-clay ceramic waste as cement mortars components. Construction and Building Materials, 31, 197–203. doi:10.1016/j.conbuildmat.2011.12.110

Sales, A., & Rodrigues de Souza, F. (2009). Concretes and mortars recycled with water treatment sludge and construction and demolition rubble. Construction and Building Materials, 23(6), 2362–2370. doi:10.1016/j.conbuildmat.2008.11.001

Shui, Z., Xuan, D., Wan, H., & Cao, B. (2008). Rehydration reactivity of recycled mortar from concrete waste experienced to thermal treatment. Construction and Building Materials, 22(8), 1723–1729. doi:10.1016/j.conbuildmat.2007.05.012

Silva, J., Brito, J. de, & Veiga, R. (2009). Incorporation of fine ceramics in mortars. Construction and Building Materials, 23(1), 556–564. doi:10.1016/j.conbuildmat.2007.10.014

Silva, J., Brito, J. de, & Veiga, R. (2010). Recycled Red-Clay Ceramic Construction and Demolition Waste for Mortars Production. Journal of Materials in Civil Engineering, 22(3), 236–244. doi:10.1061/?ASCE?0899-1561?2010?22:3?236?

Silva, M. A. G., Silva, Z. C. G., & Simão, J. (2007). Petrographic and mechanical aspects of accelerated ageing of polymeric mortars. Cement and Concrete Composites, 29(2), 146–156. doi:10.1016/j.cemconcomp.2006.08.003

Tam, V. W. Y., Tam, C. M., & Le, K. N. (2007). Removal of cement mortar remains from recycled aggregate using pre-soaking approaches. Resources, Conservation and Recycling, 50(1), 82–101. doi:10.1016/j.resconrec.2006.05.012

Tertre, J. I. (2007). Gestión de residuos de construcción y demoliciones. Áridos reciclados. Informes de La Construcción, 59(505), 81–87. Retrieved from http://hdl.handle.net/10261/4990

Vegas, I., Azkarate, I., Juarrero, A., & Frías, M. (2009). Diseño y prestaciones de morteros de albañilería elaborados con áridos reciclados procedentes de escombro de hormigón. Materiales de Construcción, 59(295), 5–18. doi:10.3989/mc.2009.44207

Wang, G., & Tian, B. (2009). Effect of Waste Ceramic Polishing Powder on the Properties of Cement Mortars. In Energy and Environment Technology, 2009. ICEET '09. International Conference on (pp. 101–104). IEEE. doi:10.1109/ICEET.2009.31

Figure 7. a) Flexural strength of CM with respect to age, b) Evolution of hydration with the age of CM based on the flexural strength. Source: Self-elaboration.

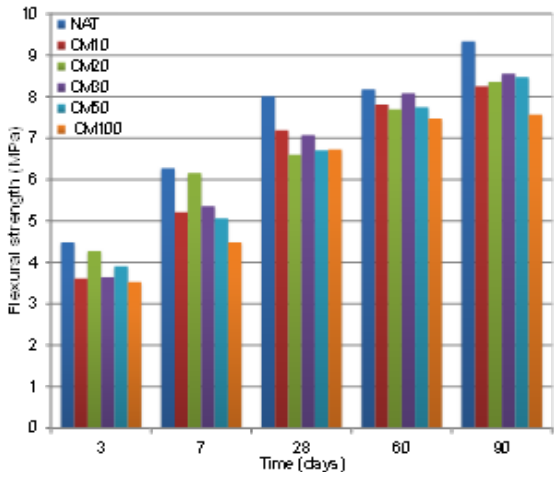

a)

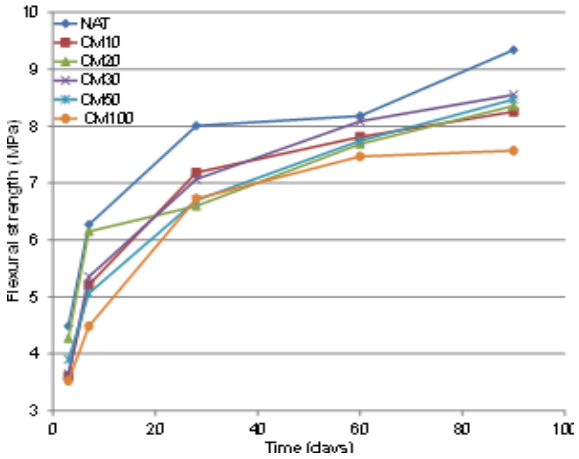

b)

Figure 8. a) εbasic, b) εtotal of the CM. Source: Self-elaboration.

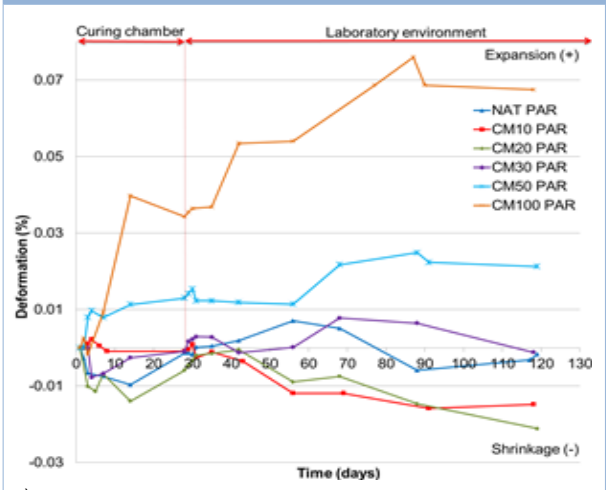

a)

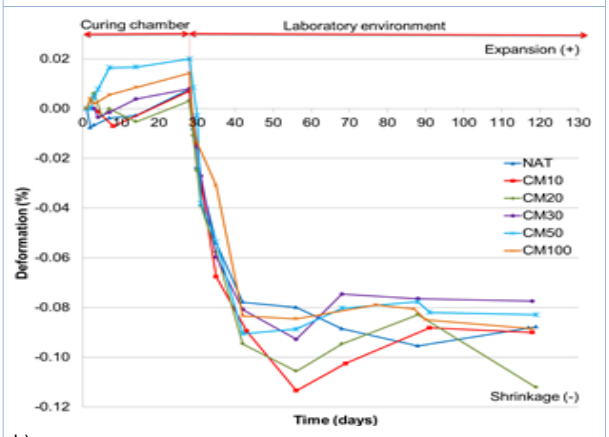

b)

Figure 9. a) εbasic, y b) εtotal for the CM in laboratory environment. Source: Self-elaboration.

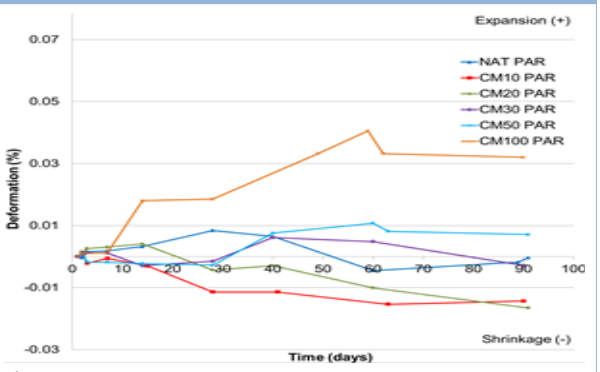

a)

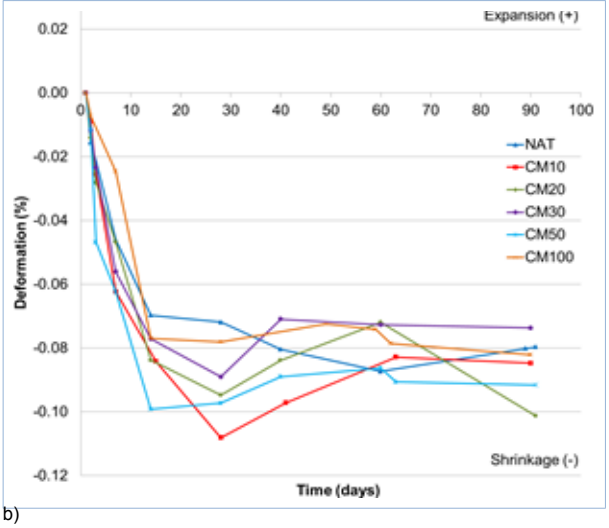

b)